

Hypoxia modulates the stem cell population and induces EMT in the MCF-10A breast epithelial cell line

CARL S. DALY¹, ARWA FLEMBAN^{1,2}, MAI SHAFEI¹, MYRA E. CONWAY¹,
DAVID QUALTROUGH¹ and SARAH J. DEAN¹

¹Department of Applied Sciences, Faculty of Health and Applied Sciences, University of West of England, Bristol, BS16 1QY, UK; ²Department of Pathology, Faculty of Medicine, Umm Al-Qura University, Makkah 24382, Saudi Arabia

DOI: 10.3892/or_XXXXXXXX

Abstract. A common feature among pre-malignant lesions is the induction of hypoxia through increased cell propagation and reduced access to blood flow. Hypoxia in breast cancer has been associated with poor patient prognosis, resistance to chemotherapy and increased metastasis. Although hypoxia HAS BEEN correlated with factors associated with the latter stages of cancer progression, it is not well documented how hypoxia influences cells in the earliest stages of transformation. Using the immortalized MCF-10A breast epithelial cell line, we used hypoxic culture conditions to mimic reduced O₂ levels found within early pre-malignant lesions and assessed various cellular parameters. In this non-transformed mammary cell line, O₂ deprivation led to some changes not immediately associated with cancer progression, such as decreased proliferation, cell cycle arrest and increased apoptosis. In contrast, hypoxia did induce other changes more consistent with an increased metastatic potential. A rise in the CD44⁺CD24⁻/low-labeled cell sub-population along with increased colony forming capability indicated an expanded stem cell population. Hypoxia also induced cellular and molecular changes consistent with an epithelial-to-mesenchymal transition (EMT). Furthermore, these cells now exhibited increased migratory and invasive abilities. These results underscore the contribution of the hypoxic tumour microenvironment in cancer progression and dissemination.

Introduction

Breast cancer is the most common malignancy in woman worldwide, and the second leading cause of cancer-related deaths in females (1). Considering that metastasis is responsible

for 90% of these deaths (2), understanding the mechanisms which contribute to this endpoint is fundamental in the design of treatment strategies to alleviate breast cancer mortality. The pathological progression of breast cancer is well documented (3). However, the factors which govern this progression are less characterized (4). Considerable attention has been paid to the contribution of somatic mutation and epigenetic alterations in cancer initiation and progression (5-7). However, the role of tumour-associated microenvironmental changes may be equally contributive and are only recently gaining impetus (8).

Hypoxia exemplifies one microenvironmental change associated with tumourigenesis. In the earliest stages of tumour development, abnormal proliferation and accumulation of cells can lead to increased cellular mass, elevated intra-tissue pressure, insufficient perfusion and subsequent O₂ deficiency (9). In breast cancer patients, intra-tumour measurements conducted *in situ* have revealed substantial levels of O₂ deprivation compared to normal breast tissue (10). Hypoxia in breast cancer has been associated with poor patient prognosis (11-13), resistance to chemotherapy (14,15) and increased metastasis (13,16,17).

How hypoxia influences cancer progression is not fully defined. It is known that cells respond to reduced O₂ availability by increasing the activity of hypoxia-inducible factors (HIF-1 α and HIF-2 α) which, in turn, mediate global transcriptional changes (18). These transcriptional changes involve many genes and may alter various cellular processes which contributes to cancer progression (18). Numerous studies connecting hypoxia and cancer have been conducted on transformed cells isolated from animal models, patient tumours and established cancer cell lines (19). However, these cells harbour many cancer-associated genetic and epigenetic changes. How hypoxia affects breast epithelial cells in the earlier stages of transformation remains less well defined.

In the present study, we used the untransformed MCF-10A breast epithelial cell line and hypoxic culture conditions to replicate conditions found within early hyperplastic breast lesions. Using this model we were able to study the effects of O₂ deprivation independent from the contribution of cancer-associated genetic and epigenetic changes. We demonstrated that reduced O₂ availability induced a number of changes consistent with increased metastatic potential. Proliferation and

Correspondence to: Dr Carl S. Daly, Department of Applied Sciences, Faculty of Health and Applied Sciences, Frenchay Campus, Coldharbour Lane, Bristol, BS16 1QY, UK
E-mail: carl.daly@uwe.ac.uk

Key words: breast, cancer, stem cells, hypoxia, MCF-10A, EMT

cell cycle progression were perturbed along with an increase in apoptosis. A rise in the CD44⁺CD24⁻/low cells coupled with an increased colony forming ability indicated a rise in the stem cell population. Cells underwent cellular and molecular changes consistent with epithelial-to-mesenchymal transition (EMT). Furthermore, hypoxia increased the migratory and invasive capabilities of these cells. Collectively, these results highlight the contribution of hypoxic microenvironmental changes in cancer progression and dissemination.

Materials and methods

Human tissue samples and ethics statement. Surplus breast tissue initially removed surgically for diagnostic purposes was used in the present study following informed patient consent. Archived paraffin-embedded tissue was obtained from Bristol Royal Infirmary under ethical approval from the NHS Health Research Authority and UWE Ethics Committee (Ref. 11/SW/0127). All methods were performed in accordance with the NHS Health Research Authority guidelines and regulations.

Cell culture and hypoxia. MCF-10A cells were purchased from the American Tissue Culture Collection (ATCC; Manassas, VA, USA) and cultured in Dulbecco's modified Eagle's medium/Nutrient Mixture F-12 Ham supplemented with 100 ng/ml cholera toxin (Sigma, St. Louis, MO, USA), 20 ng/ml epidermal growth factor (EGF) (Thermo Fisher Scientific, Inc., Waltham, MA, USA), 10 µg/ml insulin, 500 ng/ml hydrocortisone and 5% heat-inactivated horse serum (all from Sigma). Experiments were conducted in the aforementioned media mixture excluding EGF (media was replaced at least 24 h before experiments). MCF-10A cells were subjected to no >8 passages in culture before experiments. Whilst control cells were incubated at 37°C in a humidified atmosphere containing 5% CO₂ and ~21% O₂ (termed normoxia), hypoxic conditions (termed hypoxia) were induced using an airtight modular incubator chamber (Billups-Rothenberg, Inc., San Diego, CA, USA). Briefly, the cells were sealed in the modular incubator chambers with a sterile phosphate-buffered saline (PBS) reserve to maintain humidity, and then purged with a reduced O₂ gas mixture (1% O₂, 5% CO₂ and 94% N₂). The chamber was then sealed and placed in an incubator at 37°C for 72 h.

Immunofluorescence microscopy. Paraffin blocks containing embedded human breast tissue were sectioned at 4 µm using a microtome (Leica RM2235) and mounted on Superfrost Plus slides (Thermo Fisher Scientific, Inc.). Sections were then deparaffinized with Histoclear (National Diagnostics, Atlanta, GA, USA) and rehydrated using a series of ethanol concentrations and dH₂O. Antigen unmasking was performed by heating in citrate buffer (pH 6.0) using a water bath for 30 min (95-100°C) and then allowing the sections to cool to room temperature (RT) in the buffer. Cultured MCF-10A cells were fixed with ice cold 4% paraformaldehyde for 20 min and then stored at 4°C in 70% ethanol. The slides and/or fixed cells were incubated in blocking serum [goat serum (Vector Laboratories, Burlingame, CA, USA) diluted in Tris-buffered saline (TBS)] for 30 min at RT, and then incubated in a primary antibody overnight at 4°C. Antibodies used were anti-human and are as follows: CA IX

(a kind gift from Professor M. Lodomery), Ki-67 (Thermo Fisher Scientific, Inc.), cleaved caspase-3 (Cell Signaling Technology, Inc., Beverly, MA, USA), E-cadherin, β-catenin and vimentin (all from BD Biosciences, Franklin Lakes, NJ, USA). The following day, the slides and/or cells were washed in TBS and then incubated with suitable fluorescent-labelled secondary antibodies [Alexa Fluor (Thermo Fisher Scientific, Inc.)] for 1 h at RT. Subsequently, the slides and/or cells were washed with TBS, then mounted using Vectashield Hardset Mounting Media with 4,6-diamidino-2-phenylindole (DAPI) (Vector Laboratories). All images were obtained using a fluorescence microscope (Nikon Eclipse 80i).

Western blot analyses. Cells were harvested in lysis buffer (10 mM Tris-HCl, 50 mM sodium chloride, 5 mM EDTA, 15 mM sodium pyrophosphate, 50 mM sodium fluoride and 100 µM sodium orthovanadate) supplemented with phosphatase (Roche Applied Science, Indianapolis, IN, USA) and protease (Sigma) inhibitor cocktails at 4°C for 30 min. Following collection, the cells were sonicated on ice using Soniprep 150 (MSE Ltd., London, UK), then centrifuged at 15,000 x g for 15 min at 4°C and then the supernatant was collected. The protein concentration was determined using a Coomassie (Bradford) protein assay kit (Thermo Fisher Scientific, Inc.). An equal amount of protein from each sample was separated using 10% sodium dodecyl sulfate-polyacrylamide gel electrophoresis (SDS-PAGE) gel and transferred onto a nitrocellulose membrane (GE Healthcare, Little Chalfont, UK). After blocking with 5% milk powder for 1 h at room temperature, the membranes were incubated in a primary antibody overnight at 4°C. The antibodies used were anti-human and are as follows: CA IX (a gift from Professor M. Lodomery), E-cadherin, β-catenin, vimentin (all from BD Biosciences) and β-actin (Thermo Fisher Scientific, Inc.) which was used as a loading control. The blot membrane was washed, then incubated with a horseradish peroxidase-conjugated secondary antibody, and signals were revealed using a chemiluminescence kit (Thermo Fisher Scientific, Inc.).

Proliferation and apoptosis scoring. Proliferation and apoptosis were assessed as a percentage of Ki-67-positive cells and a percentage of cleaved caspase-3-positive cells, respectively. Briefly, 10 evenly distributed x40 fields of view were imaged using a fluorescence microscope (Nikon Eclipse 80i) for each independent group. Positively-labeled cells were counted and scored as a percentage of total cells. Experiments were performed at least in triplicate for each group.

Flow cytometry. Cells were washed once with Hanks' balanced salt solution (HBSS) (Thermo Fisher Scientific, Inc.), and then harvested with 0.05% trypsin/0.025% EDTA (Thermo Fisher Scientific, Inc.). Detached cells were washed with HBSS containing 2% horse serum (Sigma) (wash buffer), and re-suspended in the wash buffer (10⁶ cells/100 µl). Anti-human CD24-FITC-conjugated (BD Biosciences) and anti-human CD44-APC-conjugated (BioLegend, Inc., San Diego, CA, USA) antibodies or the respective isotype controls were added to the cell suspension, as recommended by the manufacturer, and incubated at 4°C in the dark for 30 min. Subsequently, the

1 labelled cells were washed in wash buffer and then analysed
2 on an Accuri C6 cytometer using CFlow Plus software (both
3 from BD Biosciences).

4
5 *Cell cycle analysis.* Cells were harvested, washed with ice-cold
6 PBS, and then fixed in 70% ethanol for at least 30 min at 4°C.
7 Before analysis, the cells were washed again in PBS, then
8 incubated in staining buffer [100 µg/ml RNase and 50 µg/ml
9 propidium iodide (PI) (Sigma)] in the dark at 4°C for 30 min.
10 The samples were analysed by flow cytometry using an
11 Accuri C6 cytometer (BD Biosciences). CFlow plus software
12 (BD Biosciences) was used to calculate the percentage of cells
13 in the G0/G1, S and G2/M phases. All studies were performed
14 in triplicate.

15
16 *Mammosphere forming assay.* Six-well culture plates were
17 coated with poly(2-hydroxyethyl methacrylate) (Santa Cruz
18 Biotechnology, Santa Cruz, CA, USA) to obtain an ultra-
19 low adhesion surface. Following treatment, the cells were
20 trypsinized and mechanically disrupted to obtain single-cell
21 suspensions. The single-cell suspensions were then plated at
22 1×10^3 in 1 ml MCF-10A medium in the ultra-low adhesion
23 wells. The cells were left to form spheres for 10 days, and
24 mammospheres were considered cell aggregates $>50 \mu\text{m}$ in
25 diameter. The mammospheres were imaged, counted and
26 measured using a phase-contrast inverted microscope (Nikon
27 Eclipse TE300). Each experiment was repeated in triplicate.

28
29 *Wound healing assay.* Cells were plated in 6-well culture
30 plates, and wounds were inflicted upon the cell monolayers
31 using a sterile plastic 200-µl micropipette tip. Phase-contrast
32 microscopy images were immediately obtained after
33 wounding and again 48 h later using an inverted microscope
34 (Nikon Eclipse TE300). The experiments were independently
35 performed in triplicate, and the migration distance under
36 each condition was assessed by analyzing the images using
37 ImageJ software (National Institutes of Health, Rockville,
38 MD, USA).

39
40 *Transwell invasion assay.* Transwell inserts (Millipore,
41 Billerica, MA, USA) containing polycarbonate filters with
42 8-µm pores were used in the assay. The inserts were coated
43 with 50 µl of Matrigel matrix (1 mg/ml) according to the
44 manufacturer's recommendations (Thermo Fisher Scientific,
45 Inc.). The cells were seeded in the upper chambers of the
46 inserts at a density of 2×10^5 cells in 1 ml serum-free MCF-10A
47 medium. MCF-10A medium (2 ml) containing serum was
48 placed in the lower chambers. Following 72 h of treatment,
49 the cells on the upper surface of the membrane were removed
50 using a methanol coated cotton swab. The cells on the lower
51 chamber were fixed in 4% paraformaldehyde and stained with
52 hematoxylin (Sigma). For each membrane, the number of cells
53 was counted in 10 evenly distributed x40 fields of view using
54 a light microscope (Nikon Eclipse 80i). Each experiment was
55 repeated in triplicate.

56
57 *Statistical analysis.* Data for each group are presented as the
58 mean \pm SD. Statistical analyses were performed using SPSS
59 for Windows, version 20.0 (IBM SPSS, Inc., Chicago, IL,
60 USA). Values of $P < 0.05$ were deemed statistically significant.

Results

61
62
63 *Hypoxic conditions induce upregulation of carbonic anhy-*
64 *drase (CA IX).* CA IX is a downstream target of HIF-1 α and
65 a robust marker of hypoxia (20). To assess the consequence
66 of abnormal breast cell propagation on intracellular O₂
67 levels, sections of hyperplastic breast tissue were labeled
68 for CA IX and compared to control tissue (Fig. 1A). Whilst
69 CA IX expression was undetectable in control tissue,
70 upregulation was prominent within hyperplastic tissue with
71 the highest expression observed within the center of lesions
72 corresponding to areas with the most limited access to blood
73 supply.

74 To model hypoxic conditions found within the breast
75 tumour microenvironment and delineate-associated conse-
76 quences, MCF-10A cells were cultured in hypoxic conditions
77 (1% O₂) for 72 h and compared to cells cultured in normoxia
78 (21% O₂). Previous studies have suggested a level of ~1% O₂ is
79 found within the breast tumour microenvironment (21). Whilst
80 control MCF-10A cells cultured in normoxia displayed unde-
81 tectable levels of CA IX expression, MCF-10A cells cultured
82 under hypoxic conditions displayed an increase in CA IX
83 expression detected by both fluorescence microscopy (Fig. 1B)
84 and western blot analysis (Fig. 1C).

85
86 *Hypoxia reduces proliferation, induces apoptosis and*
87 *perturbs cell cycle progression.* Increased cell division and
88 evasion of cell death are both prominent features in most
89 tumours (22). To assess the effects of hypoxia on cell division,
90 proliferation was analysed by monitoring changes in Ki-67
91 expression (Fig. 2A). A statistically significant reduction in the
92 percentage of Ki-67 positive cells was observed in MCF-10A
93 cells cultured under hypoxic conditions in comparison to those
94 cultured in normoxia (2.50 ± 1.28 compared to $29.53 \pm 3.89\%$
95 respectively; $P < 0.05$) (Fig. 2B). To assess the effects of hypoxia
96 on cell death, apoptosis was analysed using cleaved caspase-3
97 expression (Fig. 2C). A statistically significant increase in the
98 percentage of cleaved caspase-3 positive cells was observed in
99 MCF-10A cells cultured under hypoxic conditions compared
100 with those cultured in normoxia (3.91 ± 1.12 compared to
101 $0.35 \pm 0.18\%$ respectively; $P < 0.05$) (Fig. 2D).

102 Given the decrease in proliferation and increase in
103 apoptosis in MCF-10A cells cultured in hypoxia and the link
104 between these parameters and cell cycle progression, cell cycle
105 distribution analysis was performed using PI staining and
106 flow cytometry (Fig. 2E). 'Gating' was performed in analyses
107 to include live cells in the G0/G1, S or G2/M phases whilst
108 excluding debris and/or necrotic cells. MCF-10A cells cultured
109 in normoxia had the following distribution: G0/G1 phase,
110 $74.27 \pm 0.81\%$; S phase, $5.63 \pm 0.32\%$; and G2/M phase,
111 $18.57 \pm 1.30\%$, whilst MCF-10A cells cultured in hypoxia
112 had this distribution: G0/G1 phase, $63.83 \pm 1.63\%$; S phase,
113 $3.33 \pm 0.25\%$; and G2/M phase, $32.40 \pm 3.15\%$. As shown in
114 Fig. 2F, MCF-10A cells cultured in hypoxic conditions had a
115 statistically significant decrease in the percentage of cells in
116 the G0/G1 and S phases ($P < 0.05$), compared to MCF-10A cells
117 cultured in normoxia. Conversely, a statistically significant
118 increase in the percentage of cells in the G2/M phase ($P < 0.05$)
119 was observed in MCF-10A cells cultured in hypoxia compared
120 to MCF-10A cells cultured in normoxia. Collectively, these

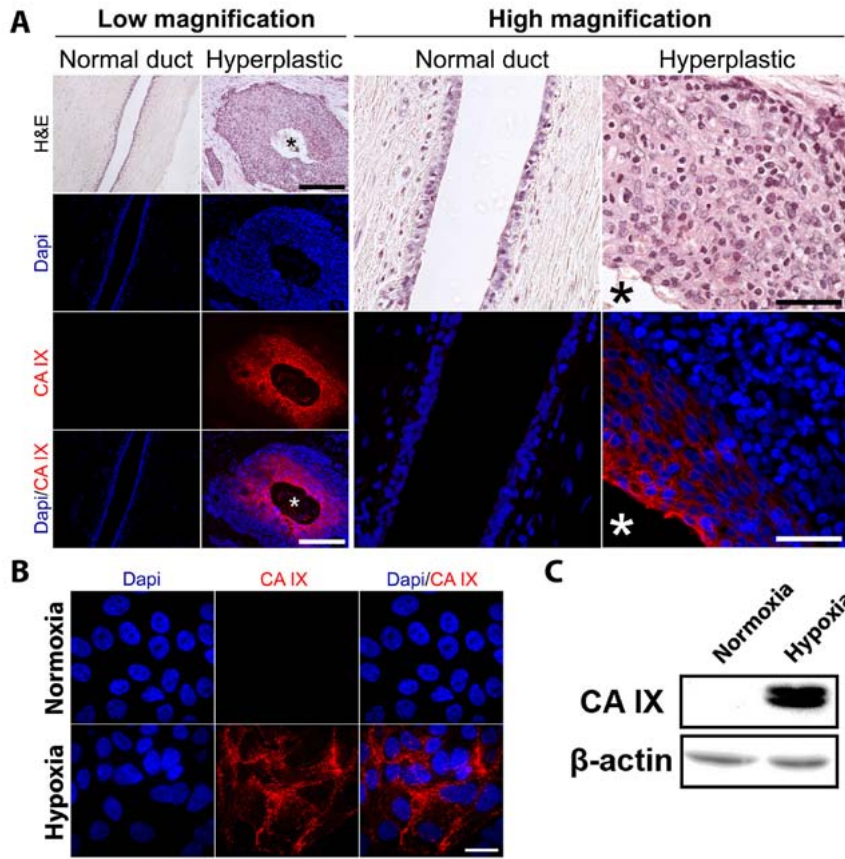


Figure 1. CA IX expression marks hypoxia in human breast tissue. (A) Serial sections of human breast tissue were stained with H&E or labeled for CA IX using fluorescent immunohistochemistry (scale bar represents 200 μ m in low magnification; 50 μ m in high magnification; * denotes the region furthest away from blood supply). (B) MCF-10A cells were placed in 20% O₂ or 1% O₂ culture conditions for 72 h then labeled for CA IX using fluorescent immunohistochemistry (scale bar represents 10 μ m). (C) The expression levels of CA IX in MCF-10A cells were detected by western blotting, β -actin served as a loading control.

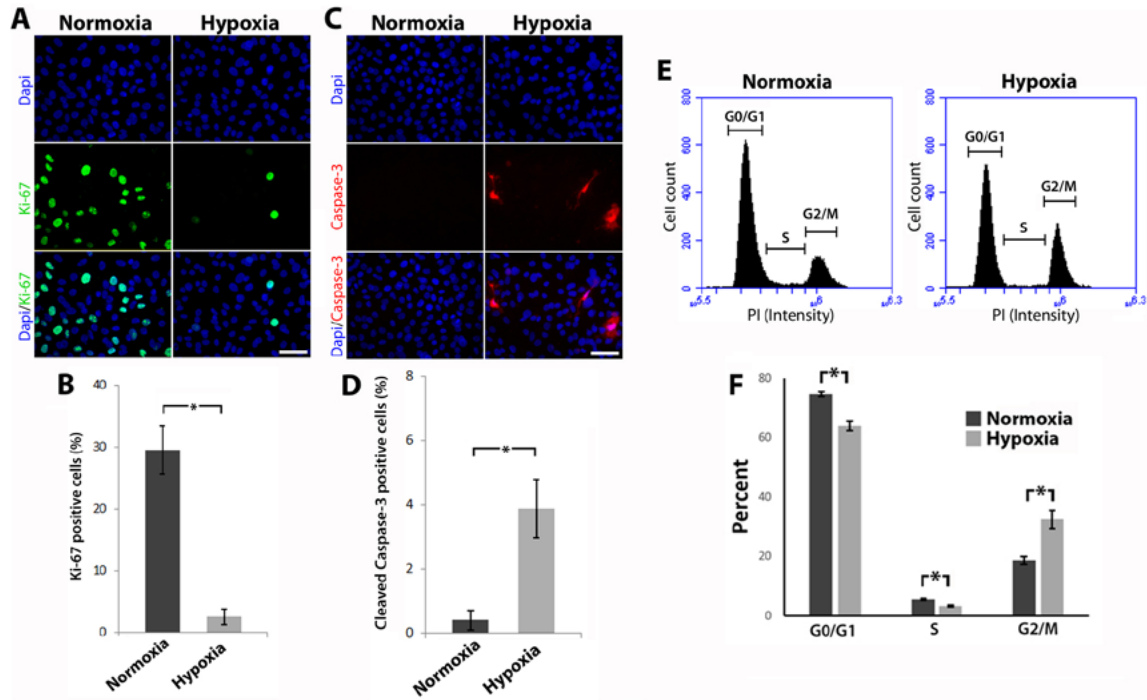


Figure 2. Hypoxia reduces proliferation, perturbs cell cycle progression and induces apoptosis. (A) Cells were labeled for Ki-67 using fluorescent immunohistochemistry (scale bar, 25 μ m). (B) Percentage of Ki-67 positive cells (error bars \pm standard deviation, * P \leq 0.05, Mann-Whitney U test, $n \geq 3$). (C) Cells were labeled for cleaved caspase-3 using fluorescent immunohistochemistry (scale bar, 25 μ m). (D) Percentage of cleaved caspase-3 positive cells (error bars \pm standard deviation, * P \leq 0.05, Mann-Whitney U test, $n \geq 3$). (E) Cell cycle distribution was evaluated using flow cytometry. (F) Graph displays the cell cycle phase expressed as a percentage of total cells (error bars \pm standard deviation, * P \leq 0.05, Mann-Whitney U test, $n \geq 3$).

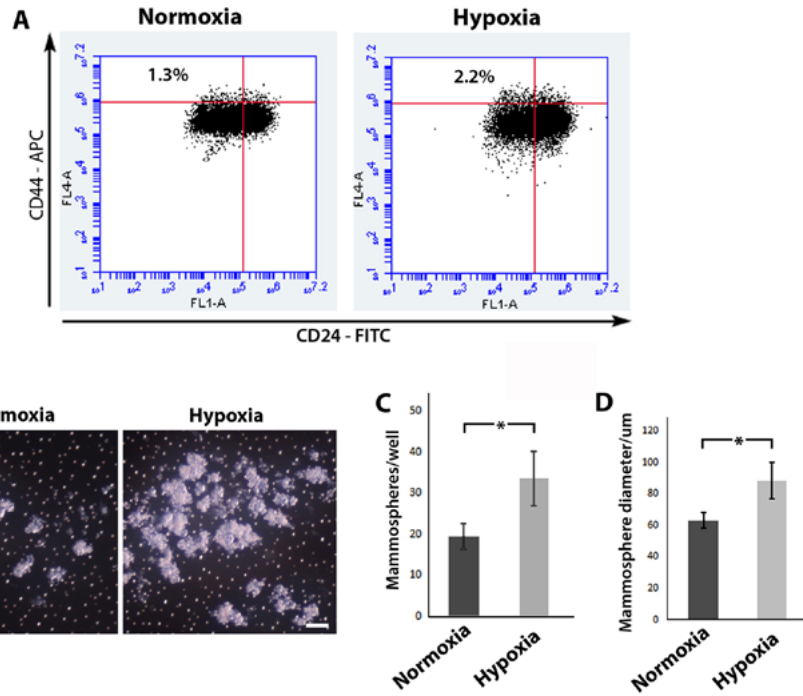


Figure 3. Hypoxia increases the stem/progenitor cell population. (A) Flow cytometric analysis of CD44 and CD24 cell surface markers. Percentage of CD44⁺CD24^{-/low} stained cells displayed. (B) Photomicrographs of mammospheres formed after 7 days (scale bar represents 100 μm). (C) Average number of mammospheres formed/well (error bars ± standard deviation, *P≤0.05, Mann-Whitney U test, n≥3). (D) Average size of formed mammospheres (error bars ± standard deviation, *P≤0.05, Mann-Whitney U test, n≥3).

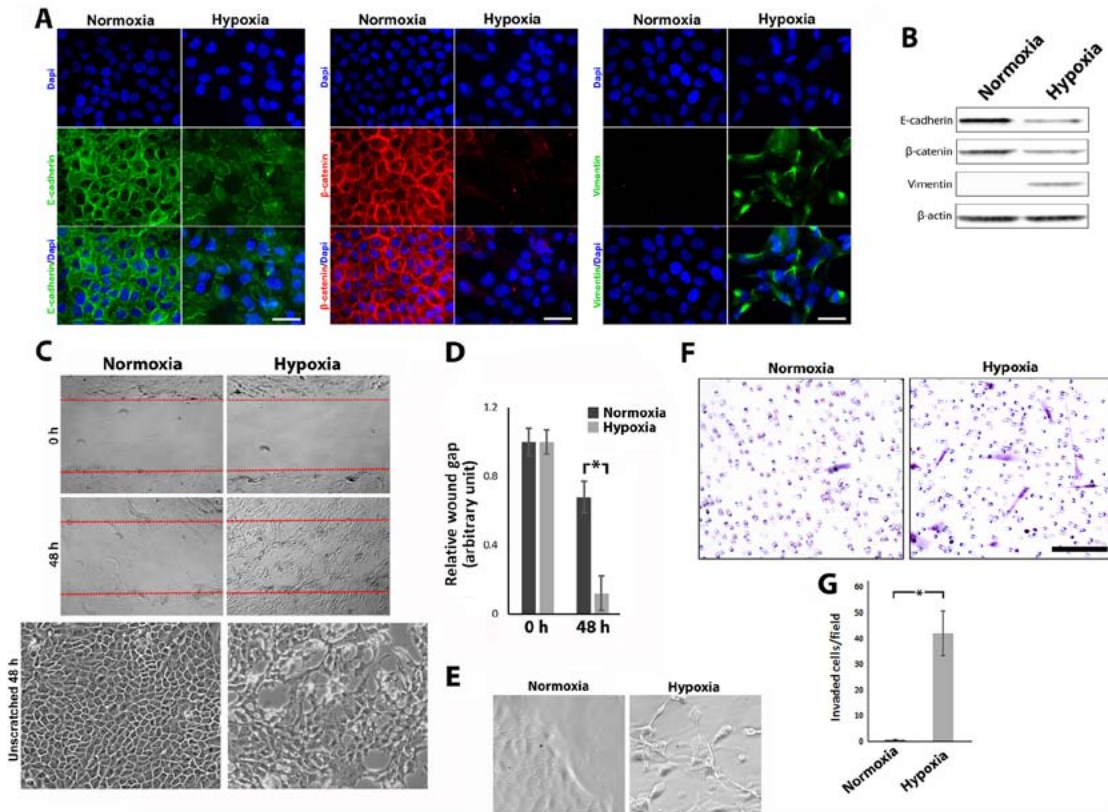


Figure 4. Hypoxia induces EMT, increased migration and invasion. (A) Cells were labeled for E-cadherin, β-catenin and vimentin using fluorescent immunohistochemistry (scale bar, 25 μm). (B) The levels of protein expression of E-cadherin, β-catenin and vimentin were detected by western blotting, β-actin served as a loading control. (C) Scratch wound migration assays were performed on confluent cells. Red dotted lines indicate the wound borders at the beginning of the assay. Lower panel displays comparative unscratched area. (D) Relative wound gap calculated as a ratio of the remaining wound gap at 48 h and the original wound gap at 0 h (error bars ± standard deviation, *P≤0.05; Mann-Whitney U test, n≥3). (E) Phase contrast images of migratory leading edge. (F) Photomicrographs of invaded cells in Matrigel Transwell assay. (G) Average number of invaded cells/field of view (error bars ± standard deviation, *P≤0.05; Mann-Whitney U test, n≥3).

1 data revealed that hypoxia can regulate cell growth and can
2 block cell cycle progression in the G2/M phase.

3
4 *Hypoxia increases the stem cell population.* Previous studies
5 have utilized the cell surface markers CD44 and CD24 to
6 distinguish a CD44⁺CD24⁻/low sub-population which is
7 enriched for stem cells/cancer stem cells (23,24). Using flow
8 cytometric analysis (Fig. 3A), we revealed that MCF-10A
9 cells cultured under hypoxic conditions displayed a higher
10 percentage of cells in the CD44⁺CD24⁻/low sub-population
11 in comparison to MCF-10A cells cultured in normoxia (2.2%
12 in comparison to 1.3%, respectively). Mammosphere assays
13 have been previously used as a surrogate reporter of stem cell
14 activity (25,26), and an increase in the number and/or size
15 of formed colonies are indicative of an expanded stem cell
16 population. MCF-10A cells grown in normoxia or hypoxia
17 were seeded in low adhesion culture vessels, left to form
18 spheres in normoxia and then compared (Fig. 3B). Following
19 re-oxygenation, MCF-10A cells cultured in hypoxia displayed
20 a statistically significant increase in both mammosphere
21 forming efficiency (33.50±6.56/well compared to 19.50±3.11/
22 well, respectively; P<0.05) (Fig. 3C) and mammosphere
23 size (88.78±11.57 compared to 63.49±4.77 μ m respectively,
24 P<0.05) (Fig. 3D) in comparison to MCF-10A cells initially
25 cultured in normoxia. Collectively, these results suggest that
26 hypoxic conditions lead to an expansion of the stem cell popu-
27 lation.

28
29 *Hypoxia induces EMT, increases migration and invasion.*
30 EMT is a process in which epithelial cells lose epithelial
31 characteristics and acquire mesenchymal properties. It is
32 recognized as an important event in the progression and
33 dissemination of cancer (27). MCF-10A cells cultured in
34 hypoxia or normoxia were labeled for E-cadherin, β -catenin and
35 vimentin using fluorescent immunohistochemistry (Fig. 4A).
36 MCF-10A cells cultured in hypoxic conditions displayed a
37 loss of total and membrane bound E-cadherin, a loss of total
38 and membrane bound β -catenin (although no nuclearization
39 was apparent) concomitant with an upregulation of vimentin
40 expression. Collectively, these expression changes along with
41 characteristic changes noticed in cell shape are indicative of
42 EMT (28,29). Total levels of protein expression, as detected
43 by western blotting, confirmed global changes (Fig. 4B).
44 Migratory and invasive capabilities are further traits acquired
45 by cells to allow cancer metastasis (30). Scratch wound assays
46 were used to assess the migratory ability of MCF-10A cells
47 cultured in hypoxia vs. normoxia (Fig. 4C). MCF-10A cells
48 cultured under hypoxic conditions displayed an increase in
49 migratory ability. Comparative unscratched areas demonstrate
50 highly polarized and tightly packed cells following normoxic
51 culture conditions whilst following hypoxia, cells lose
52 their tightly packed formation and appear more sporadic.
53 Collectively, this suggests that wound closure is due to
54 increased migratory abilities rather than an increase in cell
55 numbers. Quantitative analysis of wound gap closure (Fig. 4D)
56 revealed a statistically significant increase in gap closure and
57 thus a higher rate of migration in MCF-10A cells cultured
58 under hypoxic conditions (relative gap remaining after 48 h
59 in normoxic culture conditions 0.68±0.091 compared to
60 0.12±0.1 in cells cultured under hypoxic conditions; P<0.05).

Higher magnification of MCF-10A cells at the leading edge of
migration revealed the extent of changes in cell shape and a
more 'mesenchymal/fibroblastic' appearance of cells cultured
in hypoxia as opposed to normoxia (Fig. 4E). A Matrigel
Transwell invasion assay was used to compare and analyze
the invasive capacity of MCF-10A cells cultured in hypoxia
vs. normoxia. Whilst cells cultured in normoxia displayed
a limited ability to move across the Matrigel barrier, cells
cultured in hypoxic conditions were readily observed on the
bottom of the insert (Fig. 4F). Quantification of these cells
revealed a significant increase in the number of invaded cells
in cells cultured under hypoxic conditions in comparison to
those cultured in normoxia (42.2±8.57/field of view compared
to 0.77±0.05/field of view respectively; P<0.05). Collectively,
these results revealed that O₂ deprivation in MCF-10A cells
can lead to changes consistent with EMT, increased migratory
ability and increased invasive capabilities.

Discussion

As metastasis is responsible for ~90% of cancer-related
deaths (2), underscoring the mechanisms that contribute
to cancer dissemination are vital in our understanding of
the disease and may thus help expose potential preventative
strategies. Whilst considerable attention has been paid to
the contribution of genetic and epigenetic alterations in this
pathological process (5-7), the importance of tumour micro-
environmental changes are beginning to be exposed (8). In
the present study, we used hypoxic conditions to replicate
an important microenvironmental change associated with
tumourigenesis. MCF-10A cells were exposed to low O₂ levels
to replicate conditions found within the earlier stages of breast
tumourigenesis. O₂ deprivation led to some changes not imme-
diately associated with tumourigenesis, such as decreased
proliferation, cell cycle arrest and increased apoptosis. In
contrast, hypoxia-induced changes were more consistent with
a progression towards metastatic disease, such as an increase
in 'stemness', induction of EMT and increased migratory and
invasive capabilities.

Previous studies have linked hypoxia with reduced
proliferation in breast cancer cell lines and ductal carcinoma
in situ (31), a precursor of invasive ductal carcinoma. HIF-1 α
expression has been observed at this early stage of breast tumour
development (31,32), and has been revealed to both inhibit
transcription (33), and promote degradation (34) of c-MYC, an
essential regulator of cellular growth and the cell cycle (35).
Cell cycle progression was attenuated at the G2/M phase in
our model and may represent a further mechanism for our
observed reductions in proliferation. Previous studies have
linked hypoxia with several G2/M checkpoint regulators and
blockage of cell cycle progression at this phase (36,37) and
this has been reported to contribute to increased chemo- and/
or radio-resistance in some tumours (38,39). The induction of
apoptosis in our model may also be explained through HIF-1 α
expression. HIF-1 α has previously been reported to promote
apoptosis (40,41). This, in part, could be explained by stabili-
zation of p53 by HIF-1 α (42) and/or by increased transcription
of HIF-1 α targets which are pro-apoptotic such as NIP3 (43).

Given that sustaining proliferative signaling and resisting
cell death are 'hallmarks' of cancer (22), reduced proliferation, 120

cell cycle arrest and increased apoptosis induced by hypoxia may seem disadvantageous for tumorigenesis. However, previous studies have demonstrated that hypoxia can exert a selective pressure whereby cells with accumulated genetic alterations, such as the loss of p53 (44), gain a selective advantage and constitute the tumour (44,45). Furthermore, it is known that hypoxia can increase mutation frequency and lead to genomic instability (46). This is most likely due to the effects of hypoxia on the DNA damage response exerted through both HIF-1 α dependent (47) and HIF-1 α independent means (48). Collectively, these changes can lead to the generation of cells which possess the genetic and epigenetic adaptations essential for tumour progression into metastatic disease.

Hypoxia in our model also induced an increase in the stem cell population. The link between stem cells and cancer is well documented (49,50), and cancer stem cells are reportedly responsible for initiating metastatic growth in various cancers including breast (23,51,52). Previous studies have reported a less differentiated phenotype and/or an increase in stemness induced by hypoxia in breast tumour tissue (31,53,54). Increases in stemness can, in part, be explained by the ability of HIF-1 α and HIF-2 α to induce various transcriptional programs, some of which include pluripotency factors (55,56). The consequence of hypoxia-induced increases in stem cell numbers in early neoplastic lesions and the contribution of this to metastatic disease may be two-fold. First, an increase in stem cell numbers due to hypoxia along with the increased rate of mutation may increase the chance of oncogenic mutations occurring within stem cell populations leading to cancer stem cells. Second, hypoxia leading to an increase in the number of cancer stem cells may lead to an increase in metastatic potential. These reasons may contribute to why hypoxia is linked to increased metastatic disease (13,16,17).

A more direct involvement of hypoxia in metastasis is elucidated from the induction of EMT observed in our model along with the increased migratory and invasive behavior of these cells. As mentioned previously, EMT is an important event in the progression and dissemination of cancer (27). Previous studies have linked hypoxia, EMT, increased migration and invasion to various cancer cell lines including breast (57-59). This most likely occurs through HIF-1 α - and HIF-2 α -related transcriptional changes (60). In the present study we demonstrated that hypoxia-induced EMT, increased migratory and invasive behavior in untransformed cells. Given that metastasis occurs in the later stages of cancer progression following an accumulation of genetic and epigenetic alterations, the significance of this finding remains unclear. However, a mechanistic dissection of the roles of HIF-1 α and HIF-2 α isoforms at this early stage of transformation and the relevance of their true input warrant further investigation and should be the basis of further experiments.

To conclude, the present study provided evidence that tumour-associated microenvironmental changes have a substantial role alongside genetic and epigenetic alterations in the progression of breast cancer. Hypoxia can occur in the earliest stages of tumorigenesis and influence various cellular processes associated with metastatic potential. Although the present study uses a simplistic approach to delineate the contributions of the hypoxic microenvironment from the myriad of genetic and epigenetic alterations found in human

tumours; in reality, understanding the interactions between these co-contributors may elucidate the true factors driving metastasis in human disease.

Acknowledgements

We thank Dr Muhammed Sohail at Bristol Royal Infirmary for overseeing the cataloging and processing of human breast tissue samples. We also thank Mr. David Corry, Dr Jeff Davey and Dr Natasha McGuire for their technical support and Mr. Paul Kendrick for assistance in histology.

References

- Torre LA, Bray F, Siegel RL, Ferlay J, Lortet-Tieulent J and Jemal A: Global cancer statistics, 2012. *CA Cancer J Clin* 65: 87-108, 2015.
- Mehlen P and Puisieux A: Metastasis: A question of life or death. *Nat Rev Cancer* 6: 449-458, 2006.
- Rosen PP: *Rosen's Breast Pathology*. 3rd edition. LWW, 2008.
- Thompson A, Brennan K, Cox A, Gee J, Harcourt D, Harris A, Harvie M, Holen I, Howell A, Nicholson R, *et al*: Evaluation of the current knowledge limitations in breast cancer research: A gap analysis. *Breast Cancer Res* 10: R26, 2008.
- Vogelstein B, Papadopoulos N, Velculescu VE, Zhou S, Diaz LA Jr and Kinzler KW: Cancer genome landscapes. *Science* 339: 1546-1558, 2013.
- Baylin SB and Jones PA: A decade of exploring the cancer epigenome - biological and translational implications. *Nat Rev Cancer* 11: 726-734, 2011.
- Network CGA; Cancer Genome Atlas Network: Comprehensive molecular portraits of human breast tumours. *Nature* 490: 61-70, 2012.
- Bissell MJ and Hines WC: Why don't we get more cancer? A proposed role of the microenvironment in restraining cancer progression. *Nat Med* 17: 320-329, 2011.
- Semenza GL: Targeting HIF-1 for cancer therapy. *Nat Rev Cancer* 3: 721-732, 2003.
- Vaupel P, Höckel M and Mayer A: Detection and characterization of tumor hypoxia using pO₂ histography. *Antioxid Redox Signal* 9: 1221-1235, 2007.
- Vaupel P: Prognostic potential of the pre-therapeutic tumor oxygenation status. *Adv Exp Med Biol* 645: 241-246, 2009.
- van den Beucken T, Koch E, Chu K, Rupaimoole R, Prickaerts P, Adriaens M, Voncken JW, Harris AL, Buffa FM, Haider S, *et al*: Hypoxia promotes stem cell phenotypes and poor prognosis through epigenetic regulation of DICER. *Nat Commun* 5: 5203, 2014.
- Schindl M, Schoppmann SF, Samonigg H, Hausmaninger H, Kwasny W, Gnant M, Jakesz R, Kubista E, Birner P and Oberhuber G; Austrian Breast and Colorectal Cancer Study Group: Overexpression of hypoxia-inducible factor 1 α is associated with an unfavorable prognosis in lymph node-positive breast cancer. *Clin Cancer Res* 8: 1831-1837, 2002.
- Samanta D, Gilkes DM, Chaturvedi P, Xiang L and Semenza GL: Hypoxia-inducible factors are required for chemotherapy resistance of breast cancer stem cells. *Proc Natl Acad Sci USA* 111: E5429-E5438, 2014.
- O'Reilly EA, Gubbins L, Sharma S, Tully R, Guang MH, Weiner-Gorzel K, McCaffrey J, Harrison M, Furlong F, Kell M, *et al*: The fate of chemoresistance in triple negative breast cancer (TNBC). *BBA Clin* 3: 257-275, 2015.
- Hussain SA, Ganesan R, Reynolds G, Gross L, Stevens A, Pastorek J, Murray PG, Perunovic B, Anwar MS, Billingham L, *et al*: Hypoxia-regulated carbonic anhydrase IX expression is associated with poor survival in patients with invasive breast cancer. *Br J Cancer* 96: 104-109, 2007.
- Hiraga T, Kizaka-Kondoh S, Hirota K, Hiraoka M and Yoneda T: Hypoxia and hypoxia-inducible factor-1 expression enhance osteolytic bone metastases of breast cancer. *Cancer Res* 67: 4157-4163, 2007.
- Semenza GL: Hypoxia-inducible factors in physiology and medicine. *Cell* 148: 399-408, 2012.
- Kunz M and Ibrahim SM: Molecular responses to hypoxia in tumor cells. *Mol Cancer* 2: 23, 2003.

- 1 20. Potter C and Harris AL: Hypoxia inducible carbonic anhydrase IX, marker of tumour hypoxia, survival pathway and therapy target. *Cell Cycle* 3: 164-167, 2004.
- 2 21. Höckel M and Vaupel P: Tumor hypoxia: Definitions and current clinical, biologic, and molecular aspects. *J Natl Cancer Inst* 93: 266-276, 2001.
- 3 22. Hanahan D and Weinberg RA: Hallmarks of cancer: The next generation. *Cell* 144: 646-674, 2011.
- 4 23. Al-Hajj M, Wicha MS, Benito-Hernandez A, Morrison SJ and Clarke MF: Prospective identification of tumorigenic breast cancer cells. *Proc Natl Acad Sci USA* 100: 3983-3988, 2003.
- 5 24. Ghebeh H, Sleiman GM, Manogaran PS, Al-Mazrou A, Barhoush E, Al-Mohanna FH, Tulbah A, Al-Faqeeh K and Adra CN: Profiling of normal and malignant breast tissue show CD44^{high}/CD24^{low} phenotype as a predominant stem/progenitor marker when used in combination with Ep-CAM/CD49f markers. *BMC Cancer* 13: 289, 2013.
- 6 25. Dontu G, Abdallah WM, Foley JM, Jackson KW, Clarke MF, Kawamura MJ and Wicha MS: In vitro propagation and transcriptional profiling of human mammary stem/progenitor cells. *Genes Dev* 17: 1253-1270, 2003.
- 7 26. Diaz-Guerra E, Lillo MA, Santamaria S and Garcia-Sanz JA: Intrinsic cues and hormones control mouse mammary epithelial tree size. *FASEB J* 26: 3844-3853, 2012.
- 8 27. Thiery JP: Epithelial-mesenchymal transitions in tumour progression. *Nat Rev Cancer* 2: 442-454, 2002.
- 9 28. Blanco D, Vicent S, Elizegi E, Pino I, Fraga MF, Esteller M, Saffiotti U, Lecanda F and Montuenga LM: Altered expression of adhesion molecules and epithelial-mesenchymal transition in silica-induced rat lung carcinogenesis. *Lab Invest* 84: 999-1012, 2004.
- 10 29. Yoshida R, Kimura N, Harada Y and Ohuchi N: The loss of E-cadherin, alpha- and beta-catenin expression is associated with metastasis and poor prognosis in invasive breast cancer. *Int J Oncol* 18: 513-520, 2001.
- 11 30. Friedl P and Wolf K: Tumour-cell invasion and migration: Diversity and escape mechanisms. *Nat Rev Cancer* 3: 362-374, 2003.
- 12 31. Helczynska K, Kronblad A, Jögi A, Nilsson E, Beckman S, Landberg G and Pählman S: Hypoxia promotes a dedifferentiated phenotype in ductal breast carcinoma in situ. *Cancer Res* 63: 1441-1444, 2003.
- 13 32. Bos R, Zhong H, Hanrahan CF, Mommers EC, Semenza GL, Pinedo HM, Abeloff MD, Simons JW, van Diest PJ and van der Wall E: Levels of hypoxia-inducible factor-1 alpha during breast carcinogenesis. *J Natl Cancer Inst* 93: 309-314, 2001.
- 14 33. Koshiji M, Kageyama Y, Pete EA, Horikawa I, Barrett JC and Huang LE: HIF-1alpha induces cell cycle arrest by functionally counteracting Myc. *EMBO J* 23: 1949-1956, 2004.
- 15 34. Zhang H, Gao P, Fukuda R, Kumar G, Krishnamachary B, Zeller KI, Dang CV and Semenza GL: HIF-1 inhibits mitochondrial biogenesis and cellular respiration in VHL-deficient renal cell carcinoma by repression of C-MYC activity. *Cancer Cell* 11: 407-420, 2007.
- 16 35. Schmidt EV: The role of c-myc in cellular growth control. *Oncogene* 18: 2988-2996, 1999.
- 17 36. Ameltem O, Löffler M and Pettersen EO: Regulation of cell proliferation under extreme and moderate hypoxia: The role of pyrimidine (deoxy)nucleotides. *Br J Cancer* 70: 857-866, 1994.
- 18 37. Hasvold G, Lund-Andersen C, Lando M, Patzke S, Hauge S, Suo Z, Lyng H and Syljuåsen RG: Hypoxia-induced alterations of G2 checkpoint regulators. *Mol Oncol* 10: 764-773, 2016.
- 19 38. Sullivan R, Paré GC, Frederiksen LJ, Semenza GL and Graham CH: Hypoxia-induced resistance to anticancer drugs is associated with decreased senescence and requires hypoxia-inducible factor-1 activity. *Mol Cancer Ther* 7: 1961-1973, 2008.
- 20 39. Wouters A, Pauwels B, Lardon F and Vermorken JB: Review: Implications of in vitro research on the effect of radiotherapy and chemotherapy under hypoxic conditions. *Oncologist* 12: 690-712, 2007.
- 21 40. Carmeliet P, Dor Y, Herbert JM, Fukumura D, Brusselmans K, Dewerchin M, Neeman M, Bono F, Abramovitch R, Maxwell P, *et al*: Role of HIF-1alpha in hypoxia-mediated apoptosis, cell proliferation and tumour angiogenesis. *Nature* 394: 485-490, 1998.
- 22 41. Volm M and Koomägi R: Hypoxia-inducible factor (HIF-1) and its relationship to apoptosis and proliferation in lung cancer. *Anticancer Res* 20: 1527-1533, 2000.
- 23 42. Ravi R, Mookerjee B, Bhujwala ZM, Sutter CH, Artemov D, Zeng Q, Dillehay LE, Madan A, Semenza GL and Bedi A: Regulation of tumor angiogenesis by p53-induced degradation of hypoxia-inducible factor 1alpha. *Genes Dev* 14: 34-44, 2000.
- 24 43. Bruick RK: Expression of the gene encoding the proapoptotic Nip3 protein is induced by hypoxia. *Proc Natl Acad Sci USA* 97: 9082-9087, 2000.
- 25 44. Graeber TG, Osmanian C, Jacks T, Housman DE, Koch CJ, Lowe SW and Giaccia AJ: Hypoxia-mediated selection of cells with diminished apoptotic potential in solid tumours. *Nature* 379: 88-91, 1996.
- 26 45. Semenza GL: Hypoxia, clonal selection, and the role of HIF-1 in tumor progression. *Crit Rev Biochem Mol Biol* 35: 71-103, 2000.
- 27 46. Reynolds TY, Rockwell S and Glazer PM: Genetic instability induced by the tumor microenvironment. *Cancer Res* 56: 5754-5757, 1996.
- 28 47. Sendoel A, Kohler I, Fellmann C, Lowe SW and Hengartner MO: HIF-1 antagonizes p53-mediated apoptosis through a secreted neuronal tyrosinase. *Nature* 465: 577-583, 2010.
- 29 48. Bindra RS and Glazer PM: Genetic instability and the tumor microenvironment: Towards the concept of microenvironment-induced mutagenesis. *Mutat Res* 569: 75-85, 2005.
- 30 49. Clevers H: The cancer stem cell: Premises, promises and challenges. *Nat Med* 17: 313-319, 2011.
- 31 50. Visvader JE and Stingl J: Mammary stem cells and the differentiation hierarchy: Current status and perspectives. *Genes Dev* 28: 1143-1158, 2014.
- 32 51. Oskarsson T, Battle E and Massagué J: Metastatic stem cells: Sources, niches, and vital pathways. *Cell Stem Cell* 14: 306-321, 2014.
- 33 52. Velasco-Velázquez MA, Popov VM, Lisanti MP and Pestell RG: The role of breast cancer stem cells in metastasis and therapeutic implications. *Am J Pathol* 179: 2-11, 2011.
- 34 53. Keith B and Simon MC: Hypoxia-inducible factors, stem cells, and cancer. *Cell* 129: 465-472, 2007.
- 35 54. Conley SJ, Gheordunescu E, Kakarala P, Newman B, Korkaya H, Heath AN, Clouthier SG and Wicha MS: Antiangiogenic agents increase breast cancer stem cells via the generation of tumor hypoxia. *Proc Natl Acad Sci USA* 109: 2784-2789, 2012.
- 36 55. Mathieu J, Zhang Z, Nelson A, Lamba DA, Reh TA, Ware C and Ruohola-Baker H: Hypoxia induces re-entry of committed cells into pluripotency. *Stem Cells* 31: 1737-1748, 2013.
- 37 56. Zhang C, Samanta D, Lu H, Bullen JW, Zhang H, Chen I, He X and Semenza GL: Hypoxia induces the breast cancer stem cell phenotype by HIF-dependent and ALKBH5-mediated m⁶A-demethylation of NANOG mRNA. *Proc Natl Acad Sci USA* 113: E2047-E2056, 2016.
- 38 57. Muñoz-Nájara UM, Neurath KM, Vumbaca F and Claffey KP: Hypoxia stimulates breast carcinoma cell invasion through MT1-MMP and MMP-2 activation. *Oncogene* 25: 2379-2392, 2006.
- 39 58. Krishnamachary B, Zagzag D, Nagasawa H, Rainey K, Okuyama H, Baek JH and Semenza GL: Hypoxia-inducible factor-1-dependent repression of E-cadherin in von Hippel-Lindau tumor suppressor-null renal cell carcinoma mediated by TCF3, ZFH1A, and ZFH1B. *Cancer Res* 66: 2725-2731, 2006.
- 40 59. Lester RD, Jo M, Montel V, Takimoto S and Gonias SL: uPAR induces epithelial-mesenchymal transition in hypoxic breast cancer cells. *J Cell Biol* 178: 425-436, 2007.
- 41 60. Semenza GL: The hypoxic tumor microenvironment: A driving force for breast cancer progression. *Biochim Biophys Acta* 1863: 382-391, 2016.